Combined CDF and D0 Searches for the Standard Model Higgs Boson Decaying to Two Photons with up to 8.2 fb^{-1}

The TEVNPH Working Group*

for the CDF and D0 Collaborations

July 26, 2011

We combine results from CDF and D0's direct searches for the standard model (SM) Higgs boson (H) produced in $p\bar{p}$ collisions at the Fermilab Tevatron at $\sqrt{s} = 1.96$ TeV, focusing on the decay $H \to \gamma\gamma$. We compute upper limits on the Higgs boson production cross section times the decay branching fraction in the range $100 < m_H < 150$ GeV/c^2, and we interpret the results in the context of the standard model. We use the MSTW08 parton distribution functions and the latest theoretical cross section predictions when testing for the presence of a SM Higgs boson. With datasets corresponding to 7.0 fb^{-1} (CDF) and 8.2 fb^{-1} (D0), the 95% C.L. upper limits on Higgs boson production is a factor of 10.5 times the SM cross section for a Higgs boson mass of 115 GeV/c^2.

Preliminary Results

I. INTRODUCTION

The search for a mechanism for electroweak symmetry breaking, and in particular for a standard model (SM) Higgs boson, has been a major goal of particle physics for many years, and is a central part of the Fermilab Tevatron physics program, and also that of the Large Hadron Collider. Recently, the ATLAS and CMS Collaborations at the Large Hadron Collider have released results on searches for the standard model Higgs boson decaying to W^+W^- [1, 2], ZZ [3], and $\gamma\gamma$ [4, 5]. Both the CDF and D0 Collaborations have performed new combinations [6–8] of multiple direct searches for the SM Higgs boson. The sensitivities of these new combinations significantly exceed those of previous combinations [9, 10].

In this note, we combine the most recent results of searches for the SM Higgs boson produced in $p\bar{p}$ collisions at $\sqrt{s} = 1.96$ TeV, where the decay of the Higgs boson is restricted to pairs of photons: $H \to \gamma\gamma$. We consider all four SM production modes, gluon-gluon fusion: $gg \to H$, associated production of a Higgs boson with a W boson: $q\bar{q} \to WH$, associated production of a Higgs boson with a Z boson: $q\bar{q} \to ZH$, and vector-boson fusion: $q\bar{q} \to q'\bar{q}'H$. The CDF search [11] is performed with 7.0 fb^{-1} and the D0 search [12] is performed with 8.2 fb^{-1} of collision data.

The data for the CDF search are divided into four categories: Central-Central (CC), Central-Plug (CP), Central-Central Conversion (CC Conv), and Central-Plug conversion (CP Conv), which are based on whether the photon(s) are detected in the central electromagnetic (EM) calorimeter ($|\eta| < 1.1$) or the plug EM calorimeter ($1.2 < |\eta| < 2.8$), and whether or not one of the central photons is detected via its conversion products e^+e^-. The reconstructed mass resolution is approximately 2.8 GeV/c^2 for the CDF channels. The acceptances for Higgs boson decay are approximately 13% for the Central-Central category, 16% for the Central-Plug category, 2.9% for the Central-Central conversion category, and 1.8% for the Central-Plug Conversion category, varying by $\pm 10\%$ (relative) depending on the mass of the Higgs boson and the production mechanism. We assume the SM mixture of the production mechanisms. The discriminant variable is the reconstructed candidate mass $m_{\gamma\gamma}$, and the background is parameterized as a smooth function of $m_{\gamma\gamma}$ which is fit to the data outside of a window centered on the signal under test.

The D0 search requires events with at least two photon candidates with $E_T > 25$ GeV and $|\eta| < 1.1$. The diphoton mass resolution is ~ 3 GeV/c^2. The contribution of jets misidentified as photons is reduced by combining information sensitive to differences in the energy deposition from these particles in the tracker, calorimeter and central preshower in a neural network. In this latest iteration of the analysis boosted decision trees, rather than the diphoton invariant mass, are used as the final discriminating variable. The transverse energies of the leading two photons along with azimuthal opening angle between them and the di-photon invariant mass and transverse momentum are used as input variables. A sizeable improvement in sensitivity beyond that achieved with the invariant mass is obtained.

II. SIGNAL PREDICTIONS AND UNCERTAINTIES

We normalize our Higgs boson signal predictions to the most recent highest-order calculations available, for all production processes considered. The largest production cross section, $\sigma(gg \to H)$, is calculated at next-to-next-to-leading order (NNLO) in QCD with soft gluon resummation to next-to-next-to-leading-log (NNLL) accuracy, and also includes two-loop electroweak effects and handling of the running b quark mass [13, 14]. The numerical values in Table I are updates [15] of these predictions with m_t set to 173.1 GeV/c^2 [16], and an exact treatment of the massive top and bottom loop corrections up to next-to-leading-order (NLO) + next-to-leading-log (NLL) accuracy. The factorization and renormalization scale choice for this calculation is $\mu_F = \mu_R = m_H$. These calculations are refinements of earlier NNLO calculations of the $gg \to H$ production cross section [17–19]. Electroweak corrections were computed in Refs. [20, 21]. Soft gluon resummation was introduced in the prediction of the $gg \to H$ production cross section in Ref. [22].

The $gg \to H$ production cross section depends strongly on the gluon parton density function, and the accompanying value of $\alpha_s(q^2)$. The cross sections used here are calculated with the MSTW08 NNLO PDF set [23], as recommended by the PDF4LHC working group [24]. We follow the PDF4LHC working group's prescription to evaluate the uncertainties on the $gg \to H$ production cross section due to the PDFs. This prescription is to evaluate the predictions of $\sigma(gg \to H)$ at NLO using the global NLO PDF sets CTEQ6.6 [25], MSTW08 [23], and NNPDF2.0 [26], and to take the envelope of the predictions and their uncertainties due to PDF+α_s for the three sets as the uncertainty range at NLO. The

TABLE I: The production cross sections and decay branching fractions for the SM Higgs boson assumed for the combination.

m_H (GeV/c^2)	$\sigma_{gg \to H}$ (fb)	σ_{WH} (fb)	σ_{ZH} (fb)	σ_{VBF} (fb)	$B(H \to \gamma\gamma)$ (%)
100	1821.8	291.90	169.8	100.1	0.159
105	1584.7	248.40	145.9	92.3	0.178
110	1385.0	212.00	125.7	85.1	0.197
115	1215.9	174.50	103.9	78.6	0.213
120	1072.3	150.10	90.2	72.7	0.225
125	949.3	129.50	78.5	67.1	0.230
130	842.9	112.00	68.5	62.1	0.226
135	750.8	97.20	60.0	57.5	0.214
140	670.6	84.60	52.7	53.2	0.194
145	600.6	73.70	46.3	49.4	0.168
150	539.1	64.40	40.8	45.8	0.137

ratio of the NLO uncertainty range to that of just MSTW08 is then used to scale the NNLO MSTW08 PDF+α_s uncertainty, to estimate a larger uncertainty at NNLO. This procedure roughly doubles the PDF+α_s uncertainty from MSTW08 at NNLO alone.

We also include uncertainties on $\sigma(gg \to H)$ due to uncalculated higher order processes by following the standard procedure of varying the factorization renormalization scales up and down together by a factor $\kappa = 2$. We treat the scale uncertainties as 100% correlated between jet categories and between CDF and D0, and also treat the PDF+α_s uncertainties in the cross section as correlated between jet categories and between CDF and D0. We treat however the PDF+α_s uncertainty as uncorrelated with the scale uncertainty.

We include all significant Higgs boson production modes in our searches. Besides gluon-gluon fusion through virtual quark loops, we include Higgs boson production in association with a W or Z vector boson, and vector boson fusion (VBF). We use the WH and ZH production cross sections computed at NNLO in Ref. [27]. This calculation starts with the NLO calculation of v2HV [28] and includes NNLO QCD contributions [29], as well as one-loop electroweak corrections [30]. We use the VBF cross section computed at NNLO in QCD in Ref. [31]. Electroweak corrections to the VBF production cross section are computed with the HAWK program [32], and are small (3% or less) for the Higgs boson mass range considered here. The VBF cross sections in Table I do not include the electroweak corrections.

In order to predict the distributions of the kinematics of Higgs boson signal events, CDF and D0 use the PYTHIA [33] Monte Carlo program, with CTEQ5L and CTEQ6L [34] leading-order (LO) parton distribution functions.

The Higgs boson decay branching fraction $Br(H \to \gamma\gamma)$ used here is obtained from the Handbook [35]. The branching fractions are computed by evaluating the partial decay widths of on-shell Higgs bosons to all possible final states allowed in the SM, and evaluating the fractions of the total decay width for each process. For all processes except $H \to W^+W^-$ and $H \to ZZ$, HDECAY [36] is used to compute the partial widths. HDECAY includes relevant higher-order QCD corrections to decays into quarks and gluons, and NLO electroweak corrections are included in the $H \to \gamma\gamma$ and $H \to gg$ processes. For $H \to W^+W^-$ and $H \to ZZ$, the Monte Carlo generator PROPHECY4F [37] is used. It computes partial widths for Higgs boson decays at NLO, including NLO QCD and electroweak corrections and all interferences, for four-fermion final states of Higgs boson decay. More details are available in Ref. [35]. The branching fraction $Br(H \to \gamma\gamma)$ is listed in Table I as a function of m_H.

III. COMBINING CHANNELS

To gain confidence that the final result does not depend on the details of the statistical formulation, we perform two types of combinations, using Bayesian and Modified Frequentist approaches, which yield limits on the Higgs boson production rate that agree within 5% at each value of m_H, and within 1% on average. Both methods rely on distributions in the final discriminants, and not just on their single integrated values. Systematic uncertainties enter

on the predicted number of signal and background events as well as on the distribution of the discriminants in each analysis ("shape uncertainties"). Both methods use likelihood calculations based on Poisson probabilities.

Both methods treat the systematic uncertainties in a Bayesian fashion, assigning a prior distribution to each source of uncertainty, parameterized by a nuisance parameter, and propagating the impacts of varying each nuisance parameter to the signal and background predictions, with all correlations included. A single nuisance parameter may affect the signal and background predictions in many bins of many different analyses. Independent nuisance parameters are allowed to vary separately within their prior distributions. Both methods use the data to constrain the values of the nuisance parameters, one by integration, the other by fitting. These methods reduce the impact of prior uncertainty in the nuisance parameters thus improving the sensitivity. Because of these constraints to the data, it is important to evaluate the uncertainties and correlations properly, and to allow independent parameters to vary separately, otherwise a fit may overconstrain a parameter and extrapolate its use improperly. The impacts of correlated uncertainties add together linearly on a particular prediction, while those of uncorrelated uncertainties are convoluted together, which is similar to adding in quadrature.

A.   Bayesian Method

Because there is no experimental information on the production cross section for the Higgs boson, in the Bayesian technique [9][38] we assign a flat prior for the total number of selected Higgs events. For a given Higgs boson mass, the combined likelihood is a product of likelihoods for the individual channels, each of which is a product over histogram bins:

$$\mathcal{L}(R,\vec{s},\vec{b}|\vec{n},\vec{\theta}) \times \pi(\vec{\theta}) = \prod_{i=1}^{N_C}\prod_{j=1}^{N_b} \mu_{ij}^{n_{ij}} e^{-\mu_{ij}}/n_{ij}! \times \prod_{k=1}^{n_{\mathrm{np}}} e^{-\theta_k^2/2} \tag{1}$$

where the first product is over the number of channels (N_C), and the second product is over N_b histogram bins containing n_{ij} events, binned in ranges of the final discriminants used for individual analyses, such as the reconstructed dijet mass or neural-network outputs. The parameters that contribute to the expected bin contents are $\mu_{ij} = R \times s_{ij}(\vec{\theta}) + b_{ij}(\vec{\theta})$ for the channel i and the histogram bin j, where s_{ij} and b_{ij} represent the expected signal and background in the bin, and R is a scaling factor applied to the signal to test the sensitivity level of the experiment. Truncated Gaussian priors are used for each of the n_{np} nuisance parameters θ_k, which define the sensitivity of the predicted signal and background estimates to systematic uncertainties. These can take the form of uncertainties on overall rates, as well as the shapes of the distributions used for combination. These systematic uncertainties can be far larger than the expected SM Higgs boson signal, and are therefore important in the calculation of limits. The truncation is applied so that no prediction of any signal or background in any bin is negative. The posterior density function is then integrated over all parameters (including correlations) except for R, and a 95% credibility level upper limit on R is estimated by calculating the value of R that corresponds to 95% of the area of the resulting distribution.

B.   Modified Frequentist Method

The Modified Frequentist technique relies on the $\mathrm{CL_s}$ method, using a log-likelihood ratio (LLR) as test statistic [7]:

$$LLR = -2\ln \frac{p(\mathrm{data}|H_1)}{p(\mathrm{data}|H_0)}, \tag{2}$$

where H_1 denotes the test hypothesis, which admits the presence of SM backgrounds and a Higgs boson signal, while H_0 is the null hypothesis, for only SM backgrounds. The probabilities p are computed using the best-fit values of the nuisance parameters for each pseudo-experiment, separately for each of the two hypotheses, and include the Poisson probabilities of observing the data multiplied by Gaussian priors for the values of the nuisance parameters. This

technique extends the LEP procedure [38] which does not involve a fit, in order to yield better sensitivity when expected signals are small and systematic uncertainties on backgrounds are large [39].

The $\mathrm{CL_s}$ technique involves computing two p-values, $\mathrm{CL_{s+b}}$ and $\mathrm{CL_b}$. The latter is defined by

$$1 - \mathrm{CL_b} = p(LLR \leq LLR_{\mathrm{obs}}|H_0), \tag{3}$$

where LLR_{obs} is the value of the test statistic computed for the data. $1 - \mathrm{CL_b}$ is the probability of observing a signal-plus-background-like outcome without the presence of signal, i.e. the probability that an upward fluctuation of the background provides a signal-plus-background-like response as observed in data. The other p-value is defined by

$$\mathrm{CL_{s+b}} = p(LLR \geq LLR_{\mathrm{obs}}|H_1), \tag{4}$$

and this corresponds to the probability of a downward fluctuation of the sum of signal and background in the data. A small value of $\mathrm{CL_{s+b}}$ reflects inconsistency with H_1. It is also possible to have a downward fluctuation in data even in the absence of any signal, and a small value of $\mathrm{CL_{s+b}}$ is possible even if the expected signal is so small that it cannot be tested with the experiment. To minimize the possibility of excluding a signal to which there is insufficient sensitivity (an outcome expected 5% of the time at the 95% C.L., for full coverage), we use the quantity $\mathrm{CL_s} = \mathrm{CL_{s+b}}/\mathrm{CL_b}$. If $\mathrm{CL_s} < 0.05$ for a particular choice of H_1, that hypothesis is deemed to be excluded at the 95% C.L. In an analogous way, the expected $\mathrm{CL_b}$, $\mathrm{CL_{s+b}}$ and $\mathrm{CL_s}$ values are computed from the median of the LLR distribution for the background-only hypothesis.

Systematic uncertainties are included by fluctuating the predictions for signal and background rates in each bin of each histogram in a correlated way when generating the pseudo-experiments used to compute $\mathrm{CL_{s+b}}$ and $\mathrm{CL_b}$.

C. Systematic Uncertainties

Systematic uncertainties differ between experiments and analyses, and affect the rates and shapes of the predicted signal and background in correlated ways. The combined results incorporate the sensitivity of predictions to values of nuisance parameters, and include correlations between rates and shapes, between signals and backgrounds, and between channels within experiments and between experiments. More discussion on this topic can be found in the individual analysis notes [11] and [12]. Here we describe only the largest contributions and correlations between and within the two experiments.

1. Correlated Systematics between CDF and D0

The uncertainties on the measurements of the integrated luminosities are 6% (CDF) and 6.1% (D0). Of these values, 4% arises from the uncertainty on the inelastic $p\bar{p}$ scattering cross section, which is correlated between CDF and D0.

In both CDF and D0's $H \rightarrow \gamma\gamma$ analyses, the dominant background yields are calibrated with data control samples, and thus the systematic uncertainties on the background rates and shapes are considered uncorrelated between the two collaborations' results.

The theoretical cross section uncertainties on the inclusive $gg \rightarrow H$ production cross section ($\sim 14\%$), the WH and ZH cross sections ($\sim 6\%$), and the VBF cross section ($\sim 5\%$) are shared between CDF and D0 and are used in the computation of the limits scaled to the SM prediction, but are not used in the calculation of the limit on $\sigma(p\bar{p} \rightarrow H) \times Br(H \rightarrow \gamma\gamma)$.

2. Correlated Systematic Uncertainties for CDF

The dominant systematic uncertainties for the CDF analysis are shown in Table II. Each source induces a correlated uncertainty across all CDF channels' signal and background contributions which are sensitive to that source.

3. Correlated Systematic Uncertainties for D0

The dominant systematic uncertainties for the D0 analysis are shown in Table III.

TABLE II: Systematic uncertainties on the signal contributions for CDF's $H \to \gamma\gamma$ channels. Systematic uncertainties are listed by name; see the original references for a detailed explanation of their meaning and on how they are derived. Uncertainties are relative, in percent, and are symmetric unless otherwise indicated.

CDF: $H \to \gamma\gamma$ channel relative uncertainties (%)

Channel	CC	CP	CC Conv	CP Conv
	Systematic Uncertainties on Signal (%)			
Luminosity	6	6	6	6
$\sigma_{ggH}/\sigma_{VH}/\sigma_{VBF}$	14/7/5	14/7/5	14/7/5	14/7/5
PDF	2	2	2	2
ISR	3	4	2	5
FSR	3	4	2	5
Energy Scale	0.2	0.8	0.1	0.8
Trigger Efficiency	–	–	0.1	0.4
z Vertex	0.2	0.2	0.2	0.2
Conversion ID	–	–	7	7
Detector Material	0.4	3.0	0.2	3.0
Photon/Electron ID	1.0	2.8	1.0	2.6
Run Dependence	3.0	2.5	1.5	2.0
Data/MC Fits	0.4	0.8	1.5	2.0
	Systematic Uncertainties on Background (%)			
Fit Function	3.5	1.1	7.5	3.5

TABLE III: Systematic uncertainties on the signal and background contributions for D0's $H \to \gamma\gamma$ channel. Systematic uncertainties for the Higgs signal shown in this table are obtained for $m_H = 125$ GeV/c^2. Systematic uncertainties are listed by name; see the original references for a detailed explanation of their meaning and on how they are derived. Uncertainties are relative, in percent, and are symmetric unless otherwise indicated.

D0: $H \to \gamma\gamma$ channel relative uncertainties (%)

Contribution	Background	Signal
Luminosity	6	6
Acceptance	–	2
electron ID efficiency	2	–
electron track-match inefficiency	10	–
Photon ID efficiency	3	3
Photon energy scale	2	1
Cross Section	4	10
Background subtraction	8	-

IV. COMBINED RESULTS

Using the combination procedures outlined in Section III, we extract limits on SM Higgs boson production $\sigma \times B(H \to \gamma\gamma)$ in $p\bar{p}$ collisions at $\sqrt{s} = 1.96$ TeV for $100 \leq m_H \leq 150$ GeV/c^2. To facilitate comparisons with the SM and to accommodate analyses with different degrees of sensitivity, we present our results in terms of the ratio of obtained limits to the SM Higgs boson production cross section, as a function of Higgs boson mass, for test masses arranged in 5 GeV/c^2 steps between 100 and 150 GeV/c^2.

The ratios of the 95% C.L. expected and observed limit to the SM cross section are shown in Figure 1 for the combined CDF and D0 analyses. The observed and median expected ratios computed using the Bayesian and the CL$_s$ methods are listed for the tested Higgs boson masses in Table IV. In the following summary we quote only the limits obtained with the Bayesian method, which was chosen *a priori*. We obtain the observed (expected) values of 7.2 (10.6) at $m_H = 100$ GeV/c^2, 10.5 (8.5) at $m_H = 115$ GeV/c^2, and 13.4 (8.3) at $m_H = 120$ GeV/c^2.

We also compute limits on the inclusive production cross section times the decay branching ratio $\sigma(p\bar{p} \to H + X) \times Br(H \to \gamma\gamma)$, in order to reduce model dependence from the SM predictions of the cross section and the decay branching ratio. Some residual model dependence remains, however, as the SM ratios of WH, ZH, VBF, and $gg \to H$ production are assumed in order to compute the signal acceptances for each channel. The signal acceptances vary by no more than a relative 10% between the different production mechanisms, however, and so the sensitivity to the predicted ratios is small. We perform the combination calculation for this result without the theoretical uncertainties on the total production cross section and the decay branching fraction $Br(H \to \gamma\gamma)$. The resulting limits are shown in Figure 2 and listed in Table V.

TABLE IV: Ratios of median expected and observed 95% C.L. limit to the SM cross section prediction for the combined CDF and D0 analyses as a function of the Higgs boson mass in GeV/c^2, obtained with the Bayesian and CL$_s$ methods.

Bayesian	100	105	110	115	120	125	130	135	140	145	150
Expected	10.6	9.2	8.7	8.5	8.3	8.2	8.9	9.6	10.8	12.7	16.4
Observed	7.2	11.7	7.6	10.5	13.4	11.3	13.3	11.0	11.1	10.4	13.0

CL$_s$	100	105	110	115	120	125	130	135	140	145	150
Expected:	10.5	9.3	8.9	8.5	8.2	8.2	8.7	9.4	10.7	12.9	16.7
Observed:	7.0	11.7	7.6	10.5	13.3	11.3	13.5	11.1	11.2	10.2	12.7

TABLE V: The 95% CL limit on the product of the inclusive Higgs boson production cross section and the decay branching ratio to a pair of photons $\sigma(p\bar{p} \to H + X) \times Br(H \to \gamma\gamma)$, as a function of the Higgs boson mass, assuming SM ratios of the four production mechanisms.

Bayesian	100	105	110	115	120	125	130	135	140	145	150
Expected (fb)	40.1	33.7	31.7	28.2	25.5	23.2	21.5	19.5	18.2	16.4	15.6
Observed (fb)	27.2	42.6	26.8	34.9	42.0	31.9	32.6	22.5	18.6	13.6	12.4

In summary, we combine CDF and D0 results on SM Higgs boson searches with $H \to \gamma\gamma$, based on 7.0 fb^{-1} of data from CDF and 8.2 fb^{-1} of data from D0. We use the recommendation of the PDF4LHC working group for the central value of the parton distribution functions and uncertainties [24]. We use the highest-order calculations available for the $gg \to H$, WH, ZH, and VBF theoretical cross sections when comparing our limits to the SM predictions. We include consensus estimates of the theoretical uncertainties on these production cross sections and the decay branching fractions in the computations of our limits.

The 95% C.L. upper limit on Higgs boson production is a factor of 10.5 times the SM cross section for a Higgs boson mass of $m_H = 115$ GeV/c^2. Based on simulation, the corresponding median expected upper limit is 8.5 times

the SM cross section. Standard Model branching ratios, calculated as functions of the Higgs boson mass, are assumed. The results presented here extend significantly the sensitivity of the separate CDF and D0 results.
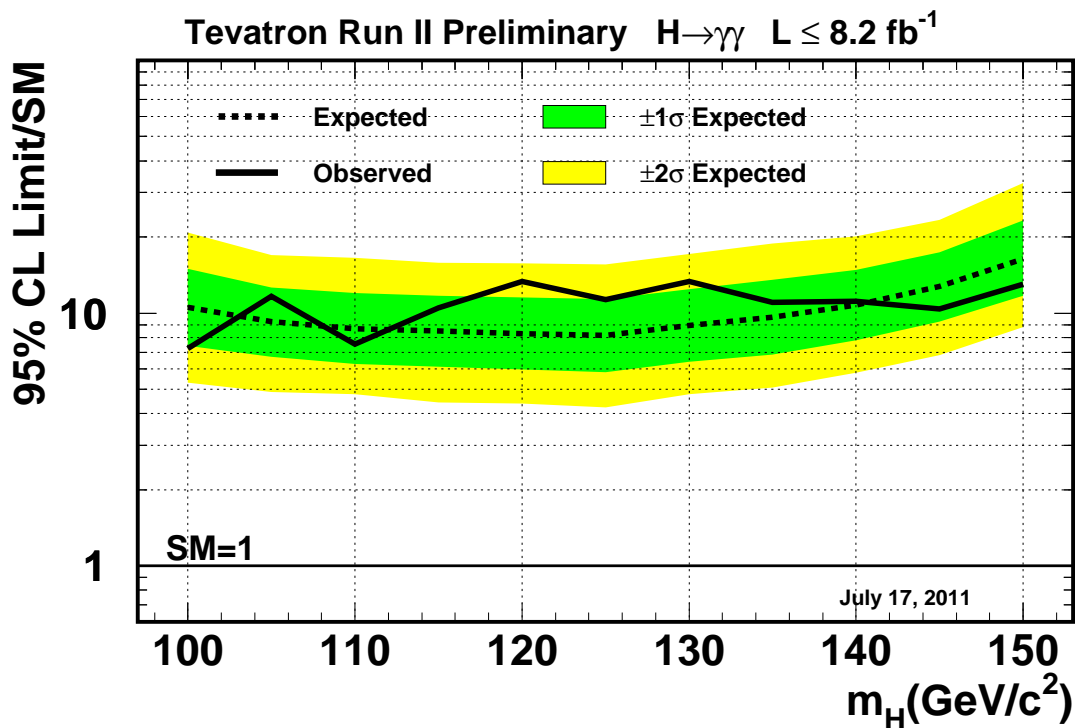
Acknowledgments

FIG. 1: Observed and expected (median, for the background-only hypothesis) 95% C.L. upper limits on the ratios to the SM cross section, as functions of the Higgs boson mass for the combined CDF and D0 analyses. The limits are expressed as a multiple of the SM prediction for test masses (every 5 GeV/c^2) for which both experiments have performed dedicated searches in different channels. The points are joined by straight lines for better readability. The bands indicate the 68% and 95% probability regions where the limits can fluctuate, in the absence of signal. The limits displayed in this figure are obtained with the Bayesian calculation.
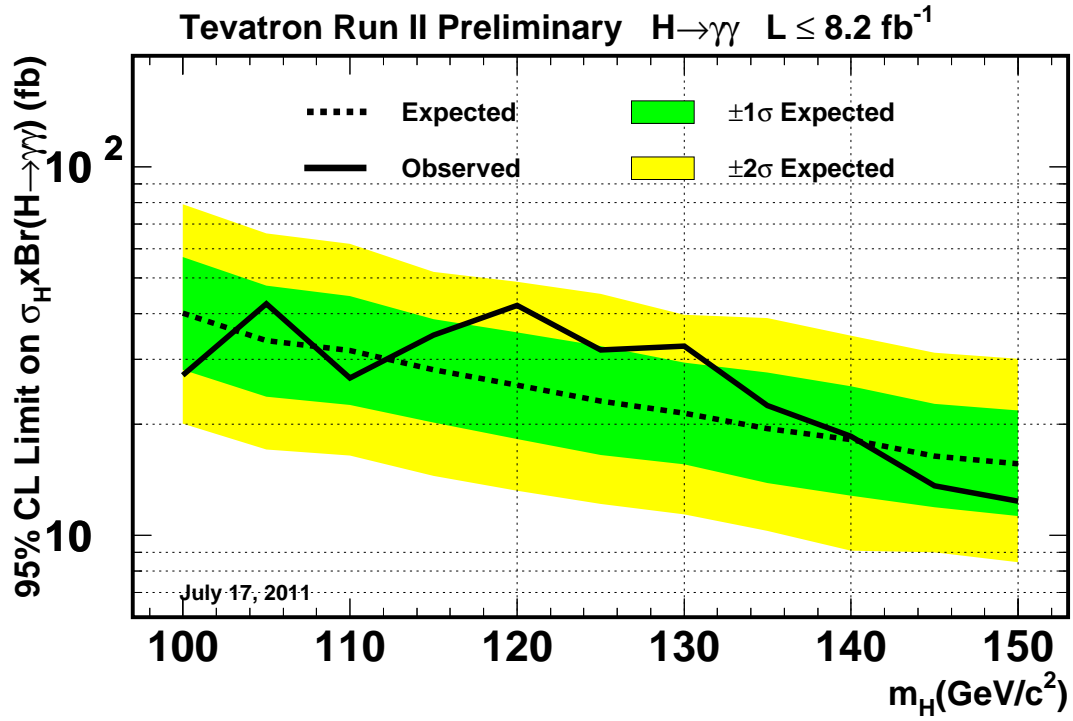
FIG. 2: Limits on the product of the inclusive Higgs boson production cross section and the decay branching ratio to a pair of photons $\sigma(p\bar{p} \to H + X) \times Br(H \to \gamma\gamma)$, as a function of the Higgs boson mass, assuming SM ratios of the four production mechanisms. The bands indicate the 68% and 95% probability regions where the limits can fluctuate, in the absence of signal.

[1] ATLAS Collaboration, "Higgs Boson Searches using the $H \to WW^{(*)} \to \ell\nu\ell\nu$ Decay Mode with the ATLAS Detector at 7 TeV", ATLAS-CONF-2011-005 (2011).

[2] CMS Collaboration, "Measurement of W+W- Production and Search for the Higgs Boson in pp Collisions at sqrt(s) = 7 TeV," [arXiv:1102.5429 [hep-ex]] (2011).

[3] ATLAS Collaboration, "Search for a Standard Model Higgs Boson in the Mass Range 200-600 GeV in the Channels $H \to ZZ \to \ell^+\ell^-\nu\bar{\nu}$ and $H \to ZZ \to \ell^+\ell^- q\bar{q}$ with the ATLAS Detector", ATLAS-CONF-2011-026 (2011).

[4] ATLAS Collaboration, "Search for the Higgs boson in the diphoton final state with 37.6 pb^{-1} of data recorded by the ATLAS detector in proton-proton collisions at $\sqrt{s} = 7$ TeV", ATLAS-CONF-2011-025 (2011).

[5] ATLAS Collaboration, "Update of the Background Studies in the Search for the Higgs Boson in the Two Photons Channel in pp Collisions at $\sqrt{s}$=7 TeV", ATLAS-CONF-2011-071 (2011).

[6] CDF Collaboration, "Search for $H \to WW^*$ Production Using 7.1 fb^{-1}", CDF Conference Note 10432 (2011).

[7] D0 Collaboration, "Combined Upper Limits on Standard Model Higgs Boson Production in the W^+W^-, $\tau\tau$ and $\gamma\gamma$ decay modes from the D0 Experiment in up to 8.2 fb^{-1} of data", D0 Conference Note 6183 (2011).

[8] The CDF and D0 Collaborations and the TEVNPHWG Working Group, "Combined CDF and D0 Upper Limits on Standard Model Higgs-Boson Production with up to 8.2 fb^{-1} of Data", FERMILAB-CONF-11-044-E, CDF Note 10441, D0 Note 6184, arXiv:1103.3233v2 [hep-ex] (2011).

[9] The CDF and D0 Collaborations and the TEVNPHWG Working Group, "Combined CDF and D0 Upper Limits on Standard Model Higgs-Boson Production with up to 6.7 fb^{-1} of Data", FERMILAB-CONF-10-257-E, CDF Note 10241, D0 Note 6096, arXiv:1007.4587v1 [hep-ex] (2010);
CDF Collaboration, "Combined Upper Limit on Standard Model Higgs Boson Production for ICHEP 2010", CDF Conference Note 10241 (2010);
D0 Collaboration, "Combined Upper Limits on Standard Model Higgs Boson Production from the D0 Experiment in up to 6.7 fb^{-1} of data", D0 Conference Note 6094 (2010).
The CDF and D0 Collaborations and the TEVNPHWG Working Group, "Combined CDF and DZero Upper Limits on Standard Model Higgs-Boson Production with 2.1 to 5.4 fb^{-1} of Data", FERMILAB-PUB-09-0557-E, CDF Note 9998, D0 Note 5983, arXiv:0911.3930v1 [hep-ex] (2009);
CDF Collaboration, "Combined Upper Limit on Standard Model Higgs Boson Production for HCP 2009", CDF Conference Note 9999 (2009);
D0 Collaboration,"Combined Upper Limits on Standard Model Higgs Boson Production from the D0 Experiment in 2.1-5.4 fb^{-1}", D0 Conference Note 6008 (2009).

[10] CDF Collaboration, "Inclusive Search for Standard Model Higgs Boson Production in the WW Decay Channel Using the CDF II Detector", Phys. Rev. Lett. 104, 061803 (2010);
D0 Collaboration, " Search for Higgs Boson Production in Dilepton and Missing Energy Final States with 5.4 fb^{-1} of $p\bar{p}$ Collisions at $\sqrt{s} = 1.96$ TeV", Phys. Rev. Lett. 104, 061804 (2010);
The CDF and D0 Collaborations, "Combination of Tevatron Searches for the Standard Model Higgs Boson in the W^+W^- Decay Mode", Phys. Rev. Lett. 104, 061802 (2010).

[11] CDF Collaboration, "Search for a Standard Model Higgs Boson Decaying Into Photons at CDF Using 7.0 fb^{-1} of Data", CDF Note 10485 (2011).

[12] D0 Collaboration, "Search for the standard model and a fermiophobic Higgs boson in diphoton final states", [e-Print: arXiv:1107.4587 [hep-ph]].

[13] C. Anastasiou, R. Boughezal and F. Petriello, JHEP **0904**, 003 (2009).

[14] D. de Florian and M. Grazzini, Phys. Lett. B **674**, 291 (2009).

[15] M. Grazzini, private communication (2010).

[16] The CDF and D0 Collaborations and the Tevatron Electroweak Working Group, arXiv:1007.3178 [hep-ex], arXiv:0903.2503 [hep-ex].

[17] R. V. Harlander and W. B. Kilgore, Phys. Rev. Lett. **88**, 201801 (2002).

[18] C. Anastasiou and K. Melnikov, Nucl. Phys. B **646**, 220 (2002).

[19] V. Ravindran, J. Smith, and W. L. van Neerven, Nucl. Phys. B **665**, 325 (2003).

[20] S. Actis, G. Passarino, C. Sturm, and S. Uccirati, Phys. Lett. B **670**, 12 (2008).

[21] U. Aglietti, R. Bonciani, G. Degrassi, A. Vicini, "Two-loop electroweak corrections to Higgs production in proton-proton collisions", arXiv:hep-ph/0610033v1 (2006).

[22] S. Catani, D. de Florian, M. Grazzini and P. Nason, "Soft-gluon resummation for Higgs boson production at hadron colliders," JHEP **0307**, 028 (2003) [arXiv:hep-ph/0306211].

[23] A. D. Martin, W. J. Stirling, R. S. Thorne and G. Watt, Eur. Phys. J. C **63**, 189 (2009).

[24] http://www.hep.ucl.ac.uk/pdf4lhc/;
     S. Alekhin *et al.*, (PDF4LHC Working Group), [arXiv:1101.0536v1 [hep-ph]];
     M. Botje *et al.*, (PDF4LHC Working Group), [arXiv:1101.0538v1 [hep-ph]].
[25] P. M. Nadolsky *et al.*, Phys. Rev. D **78**, 013004 (2008) [arXiv:0802.0007 [hep-ph]].
[26] R. D. Ball *et al.* [NNPDF Collaboration], Nucl. Phys. B **809**, 1 (2009) [Erratum-ibid. B **816**, 293 (2009)] [arXiv:0808.1231 [hep-ph]].
[27] J. Baglio and A. Djouadi, JHEP **1010**, 064 (2010) [arXiv:1003.4266v2 [hep-ph]].
[28] The Fortran program can be found on Michael Spira's web page http://people.web.psi.ch/∼mspira/proglist.html.
[29] O. Brein, A. Djouadi, and R. Harlander, Phys. Lett. B **579**, 149 (2004).
[30] M. L. Ciccolini, S. Dittmaier, and M. Kramer, Phys. Rev. D **68**, 073003 (2003).
[31] P. Bolzoni, F. Maltoni, S.-O. Moch, and M. Zaro, Phys. Rev. Lett. **105**, 011801 (2010) [arXiv:1003.4451v2 [hep-ph]].
[32] M. Ciccolini, A. Denner, and S. Dittmaier, Phys. Rev. Lett. **99**, 161803 (2007) [arXiv:0707.0381 [hep-ph]];
     M. Ciccolini, A. Denner, and S. Dittmaier, Phys. Rev. D **77**, 013002 (2008) [arXiv:0710.4749 [hep-ph]].
     We would like to thank the authors of the HAWK program for adapting it to the Tevatron.
[33] T. Sjöstrand, L. Lonnblad and S. Mrenna, "PYTHIA 6.2: Physics and manual," arXiv:hep-ph/0108264.
[34] H. L. Lai *et al.*, Phys. Rev D **55**, 1280 (1997).
[35] S. Dittmaier *et al.* [LHC Higgs Cross Section Working Group], "Handbook of LHC Higgs Cross Sections: 1. Inclusive Observables", arXiv:1101.0593v2 (2011).
[36] A. Djouadi, J. Kalinowski and M. Spira, Comput. Phys. Commun. **108**, 56 (1998).
[37] A. Bredenstein, A. Denner, S. Dittmaier, and M. M. Weber, Phys. Rev. D **74**, 013004 (2006);
     A. Bredenstein, A. Denner, S. Dittmaier, and M. Weber, JHEP **0702**, 080 (2007);
     A. Bredenstein, A. Denner, S. Dittmaier, A. Mück, and M. M. Weber, JHEP **0702**, 080 (2007) http://omnibus.uni-freiburg.de/~sd565/programs/prophecy4f/prophecy4f.html (2010).
[38] T. Junk, Nucl. Instrum. Meth. A **434**, 435 (1999);
     A.L. Read, "Modified Frequentist analysis of search results (the CL$_\mathrm{s}$ method)", in F. James, L. Lyons and Y. Perrin (eds.), *Workshop on Confidence Limits*, CERN, Yellow Report 2000-005, available through cdsweb.cern.ch.
[39] W. Fisher, "Systematics and Limit Calculations," FERMILAB-TM-2386-E.